

Acceleration statistics of heavy particles in turbulence

By J. BEC¹, L. BIFERALE², G. BOFFETTA³,
A. CELANI⁴, M. CENCINI⁵, A. LANOTTE⁶,
S. MUSACCHIO⁷, AND F. TOSCHI⁸

¹ CNRS Observatoire de la Côte d’Azur, B.P. 4229, 06304 Nice Cedex 4, France

² Dept. of Physics and INFN, University of Rome “Tor Vergata”,
Via della Ricerca Scientifica 1, 00133 Roma, Italy

³ Dept. of Physics and INFN, University of Torino, Via Pietro Giuria 1, 10125, Torino, Italy

⁴ CNRS, INLN, 1361 Route des Lucioles, F-06560 Valbonne, France

⁵ SMC-INFM c/o Dept. of Physics University of Rome “La Sapienza”, Piazz.le A. Moro, 2,
I-00185 Roma, Italy, and CNR-ISC via dei Taurini, 19 I-00185 Roma, Italy

⁶ CNR-ISAC, Sezione di Lecce, Str. Prov. Lecce-Monteroni km 1,200, I-73100 Lecce, Italy

⁷ Dept. of Physics, University of Rome “La Sapienza”, Piazz.le A. Moro, 2, I-00185 Roma, Italy

⁸ CNR-IAC, Viale del Policlinico 137, I-00161 Roma, Italy and
INFN, Sezione di Ferrara, via G. Saragat 1, I-44100, Ferrara, Italy

(Received 1 August 2018)

We present the results of direct numerical simulations of heavy particle transport in homogeneous, isotropic, fully developed turbulence, up to resolution 512^3 ($R_\lambda \approx 185$). Following the trajectories of up to 120 million particles with Stokes numbers, St , in the range from 0.16 to 3.5 we are able to characterize in full detail the statistics of particle acceleration. We show that: (i) The root-mean-squared acceleration a_{rms} sharply falls off from the fluid tracer value already at quite small Stokes numbers; (ii) At a given St the normalised acceleration $a_{\text{rms}}/(\epsilon^3/\nu)^{1/4}$ increases with R_λ consistently with the trend observed for fluid tracers; (iii) The tails of the probability density function of the normalised acceleration a/a_{rms} decrease with St . Two concurrent mechanisms lead to the above results: preferential concentration of particles, very effective at small St , and filtering induced by the particle response time, that takes over at larger St .

1. Introduction

Small impurities like dust, droplets or bubbles suspended in an incompressible flow are finite-size particles whose density may differ from that of the underlying fluid, and cannot thus be modelled as point-like tracers. The description of their motion must account for inertia whence the name *inertial particles*. At long times particles concentrate on singular sets evolving with the fluid motion, leading to the apparition of a strong spatial inhomogeneity dubbed *preferential concentration*. At the experimental level such inhomogeneities have been long known (see Eaton & Fessler 1994 for a review) and utilised for flow visualisation (e.g. exploiting bubble clustering inside vortex filaments). The statistical description of particle concentration is at present a largely open question with many industrial and environmental applications. We mention spray combustion in Diesel engines (Post & Abraham 2002) or some rocket propellers (Villedieu & Hylkema 2000), the formation of rain droplets in warm clouds (Pinsky & Khain 1997, Falkovich, Fouxon & Stepanov 2002,

Shaw 2003) or the coexistence of plankton species (Rothschild & Osborn 1988, Lewis & Pedley 2000). Inertial particles are also relevant to spore, pollen, dust or chemicals dispersion in the atmosphere where the diffusion by air turbulence may be even overcome by preferential clustering (Csanady 1980, Seinfeld 1986).

From the experimental side, the study of particle motion in turbulence has recently undergone rapid progress thanks to the development of effective optical and acoustical tracking techniques (La Porta *et al.* 2001, La Porta *et al.* 2002, Mordant *et al.* 2001, Warhaft, Gylfason, & Ayyalasomayajula 2005). In parallel with experimental effort, theoretical analysis (Balkovsky, Falkovich & Fouxon 2001, Falkovich & Pumir 2004, Bec, Gawedzki & Horvai 2004, Zaichik, Simonin & Alipchenkov 2003) and numerical simulations (Boivin, Simonin & Squires 1998, Reade & Collins 2000, Zhou, Wexler & Wang 2001, Chun *et al.* 2005) are paving the way to a thorough understanding of inertial particle dynamics in turbulent flows. Recently, the presence of strong inhomogeneities characterised by fractal and multifractal properties have been predicted, and found in theoretical and numerical studies of stochastic laminar flows (Balkovsky, Falkovich & Fouxon 2001, Bec, Gawedzki & Horvai 2004, Bec 2005), in two dimensional turbulent flows (Boffetta, De Lillo & Gamba 2004) and in three dimensional turbulent flows at moderate Reynolds numbers in the limit of vanishing inertia (Falkovich & Pumir 2004).

Here we present a Direct Numerical Simulations (DNS) study of particles much heavier than the carrier fluid in high-resolution turbulent flows. In particular, we shall focus on the behaviour of particle acceleration at varying both Stokes and Reynolds numbers. For fluid tracers, it is known that trapping into vortex filaments (La Porta *et al.* 2001, Biferale *et al.* 2005) is the main source of strong acceleration events. On the other hand, little is known about the acceleration statistics of heavy particles in turbulent flows, where preferential concentration may play a crucial role. Moreover, since in most applied cases it is almost impossible to perform DNS of particle transport in realistic settings, it is very important to understand acceleration statistics for building stochastic models of particle motion with and without inertia (Sawford & Guest 1991).

The material is organised as follows. In §2, we briefly recall the equations of motion of the inertial particles and summarise the DNS set up. In §3, we present and discuss the main results concerning the acceleration statistics. In §4 we discuss the acceleration statistics conditioned on the local structure of the flow. The final Section is devoted to conclusions and perspectives.

2. Heavy particle dynamics and numerical simulations

The equations of motion of a small, rigid, spherical particle immersed in an incompressible flow have been consistently derived from first principles by Maxey & Riley 1983. In the limiting case of particles much heavier than the surrounding fluid, these equations take the particularly simple form

$$\frac{d\mathbf{X}}{dt} = \mathbf{V}(t), \quad \frac{d\mathbf{V}}{dt} = -\frac{\mathbf{V}(t) - \mathbf{u}(\mathbf{X}(t), t)}{\tau_s}. \quad (2.1)$$

Here, $\mathbf{X}(t)$ denotes the particle trajectory, $\mathbf{V}(t)$ its velocity, $\mathbf{u}(\mathbf{x}, t)$ is the fluid velocity. The Stokes response time is $\tau_s = 2\rho_p a^2 / (9\rho_f \nu)$ where a is the particle radius ρ_p and ρ_f are the particle and fluid density, respectively, and ν is the fluid kinematical viscosity. The Stokes number is defined as $St = \tau_s / \tau_\eta$ where $\tau_\eta = (\nu/\epsilon)^{1/2}$ is the Kolmogorov timescale and ϵ the average rate of energy injection. Eq. (2.1) is valid for very dilute suspensions, where particle-particle interactions (collisions) and hydrodynamic coupling are not taken into account.

| R_λ | u_{rms} | ε | ν | η | L | T_E | τ_η | T_{tot} | T_{tr} | Δx | N^3 | N_t | N_p | N_{tot} |
|-------------|------------------|---------------|---------|--------|-------|-------|-------------|------------------|-----------------|------------|---------|------------------|------------------|------------------|
| 185 | 1.4 | 0.94 | 0.00205 | 0.010 | π | 2.2 | 0.047 | 14 | 4 | 0.012 | 512^3 | $5 \cdot 10^5$ | $7.5 \cdot 10^6$ | $12 \cdot 10^7$ |
| 105 | 1.4 | 0.93 | 0.00520 | 0.020 | π | 2.2 | 0.073 | 20 | 4 | 0.024 | 256^3 | $2.5 \cdot 10^5$ | $2 \cdot 10^6$ | $32 \cdot 10^6$ |
| 65 | 1.4 | 0.85 | 0.01 | 0.034 | π | 2.2 | 0.110 | 29 | 6 | 0.048 | 128^3 | $3.1 \cdot 10^4$ | $2.5 \cdot 10^5$ | $4 \cdot 10^6$ |

TABLE 1. Parameters of DNS. Microscale Reynolds number R_λ , root-mean-square velocity u_{rms} , energy dissipation ε , viscosity ν , Kolmogorov lengthscale $\eta = (\nu^3/\varepsilon)^{1/4}$, integral scale L , large-eddy Eulerian turnover time $T_E = L/u_{\text{rms}}$, Kolmogorov timescale τ_η , total integration time T_{tot} , duration of the transient regime T_{tr} , grid spacing Δx , resolution N^3 , number of trajectories of inertial particles for each Stokes N_t saved at frequency $\tau_\eta/10$, number of particles N_p per Stokes stored at frequency $10\tau_\eta$, total number of advected particles N_{tot} . Errors on all statistically fluctuating quantities are of the order of 10%.

The fluid evolves according to the incompressible Navier-Stokes equations

$$\frac{\partial \mathbf{u}}{\partial t} + \mathbf{u} \cdot \nabla \mathbf{u} = -\frac{\nabla p}{\rho_f} + \nu \Delta \mathbf{u} + \mathbf{f}, \quad (2.2)$$

where p is the pressure field and \mathbf{f} is the external energy source, $\langle \mathbf{f} \cdot \mathbf{u} \rangle = \varepsilon$.

The Navier-Stokes equations are solved on a cubic grid of size N^3 for $N = 128, 256, 512$ with periodic boundary conditions. Energy is injected by keeping constant the spectral content of the two smallest wavenumber shells (Chen *et al.* 1993). The viscosity is chosen so to have a Kolmogorov lengthscale $\eta \approx \Delta x$ where Δx is the grid spacing: this choice ensures a good resolution of the small-scale velocity dynamics. We use a fully dealiased pseudospectral algorithm with 2^{nd} order Adam-Bashforth time-stepping. The Reynolds numbers achieved are in the range $R_\lambda \in [65 : 185]$.

The equations of fluid motion are integrated until the system reaches a statistically steady state. Then, particles are seeded with homogeneously distributed initial positions and velocities equal to the local fluid velocity. Equations (2.1) and (2.2) are then advanced in parallel. A transient in particle dynamics follows, about 2–3 large scale eddy turn over time, before reaching a Lagrangian stationary statistics. It is only after this relaxation stage has completely elapsed that the real measurement starts. We followed 15 sets of inertial particles with Stokes numbers from 0.16 to 3.5. For each set, we saved the position and the velocity of N_t particles every $dt = 1/10\tau_\eta$ with a maximum number of recorded trajectories of $N_t = 5 \cdot 10^5$ for the highest resolution. Along these trajectories we also stored the velocity of the carrier fluid. At a lower frequency $\sim 10\tau_\eta$, we saved the positions and velocities of a larger number N_p of particles (up to $7.5 \cdot 10^6$ per St at the highest resolution) together with the Eulerian velocity field. We have also followed fluid tracers ($St = 0$), that evolve according to the dynamics

$$\frac{d\mathbf{x}(t)}{dt} = \mathbf{u}(\mathbf{x}(t), t), \quad (2.3)$$

in order to systematically assess the importance of the phenomenon of preferential concentration at varying both St and R_λ .

A summary of the various physical parameters is given in table 1.

3. Results and discussion

In this paper we focus on the statistics of particle acceleration $\mathbf{a}(t) = \frac{d\mathbf{V}}{dt}$. From previous studies on fluid tracers we know that acceleration statistics is very intermit-

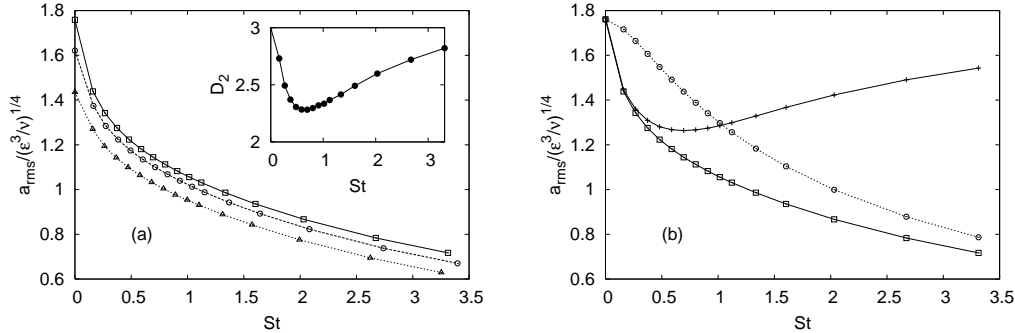


FIGURE 1. (a) The normalised acceleration variance $a_{\text{rms}}/(\epsilon^3/\nu)^{1/4}$ as a function of the Stokes number for $R_\lambda = 185$ (\square); $R_\lambda = 105$ (\circ); $R_\lambda = 65$ (\triangle). The inhomogeneous distribution of particle is quantified for the highest Reynolds in the inset, where we plot the correlation dimension, D_2 , as a function of St . The correlation dimension is defined as $p(r) \sim r^{D_2}$ (for $r \ll \eta$) where $p(r)$ is the probability to find two particles at distance smaller than r (Bec *et al.* 2005). (b) Comparison between the acceleration variance, a_{rms} (\square), as a function of Stokes and the acceleration of the fluid tracer measured on the particle position, $\langle (\frac{D\mathbf{u}}{Dt})^2 \rangle^{1/2}$ (+). The last curve (\circ), approaching the a_{rms} for large St , is the one obtained from the filtered tracer trajectories, a_{rms}^F . All data refer to $Re_\lambda = 185$.

tent and strong fluctuations are associated to trapping events within vortex filaments (La Porta *et al.* 2001, La Porta *et al.* 2002, Mordant *et al.* 2001, Biferale *et al.* 2005). How does inertia impacts acceleration statistics? A good starting point to gain insight on the effect of inertia is given by the formal solution of Eqs. (2.1) in the statistically stationary state, relating the instantaneous particle velocity to the previous history of fluid velocity along the particle trajectory. The expression is

$$\mathbf{V}(t) = \frac{1}{\tau_s} \int_{-\infty}^t e^{-(t-s)/\tau_s} \mathbf{u}(\mathbf{X}(s), s) ds \quad (3.1)$$

yielding for the acceleration

$$\mathbf{a}(t) = \frac{1}{\tau_s^2} \int_{-\infty}^t e^{-(t-s)/\tau_s} [\mathbf{u}(\mathbf{X}(t), t) - \mathbf{u}(\mathbf{X}(s), s)] ds. \quad (3.2)$$

It is instructive to analyse separately the two limiting cases of small and large Stokes numbers.

At small St , i.e. $\tau_s \ll \tau_\eta$, the fluid velocity along the trajectory evolves smoothly in time and the above expression for the acceleration reduces to $\mathbf{a}(t) \simeq \frac{d}{dt} \mathbf{u}(\mathbf{X}(t), t)$, i.e. to the derivative of fluid velocity along the inertial particle trajectory. At sufficiently small St this is indistinguishable from the fluid acceleration $\frac{D\mathbf{u}}{Dt}(\mathbf{X}(t), t)$ evaluated at particle positions. The latter, in turn, is essentially dominated by the $-\nabla p$ contribution. Therefore we are led to draw the following picture for the small St case: the heavy particle acceleration essentially coincides with the fluid acceleration; however, inertial particles are not homogeneously distributed in the flow and concentrate preferentially inside regions with relatively small pressure gradient (low vorticity regions). As a result, the net effect of inertia is a drastic reduction of the root-mean-squared acceleration $a_{\text{rms}} = \langle \mathbf{a}^2 \rangle^{1/2}$, due essentially to preferential concentration. Indeed, as shown in Fig. 1a the acceleration variance drops off very fast already at quite small St values. In Fig. 1b we give evidence that the value of a_{rms} is very close for $St < 0.4$ to $\langle (\frac{D\mathbf{u}}{Dt})^2 \rangle^{1/2}$ when the average is not taken homogeneously in space but conditioned to be on the same spatial positions of the inertial particles. The agreement of the two curves supports the arguments above. Notice

| | | | | | | | | | | | | | | | | |
|-------------------------------|------|------|------|------|------|------|------|------|------|------|------|------|------|------|------|------|
| $St^{(a)}$ | 0 | 0.16 | 0.27 | 0.37 | 0.48 | 0.59 | 0.69 | 0.80 | 0.91 | 1.01 | 1.12 | 1.34 | 1.60 | 2.03 | 2.67 | 3.31 |
| $\langle \tilde{a}^2 \rangle$ | 3.09 | 2.07 | 1.80 | 1.63 | 1.50 | 1.39 | 1.31 | 1.24 | 1.17 | 1.12 | 1.06 | 0.97 | 0.88 | 0.75 | 0.61 | 0.51 |
| $\langle \tilde{a}^4 \rangle$ | 288 | 48.1 | 30.5 | 22.4 | 17.7 | 14.5 | 12.3 | 10.6 | 9.20 | 8.11 | 7.21 | 5.77 | 4.47 | 3.11 | 1.94 | 1.29 |
| $St^{(b)}$ | 0 | 0.16 | 0.27 | 0.38 | 0.49 | 0.60 | 0.71 | 0.82 | 0.93 | 1.04 | 1.15 | 1.37 | 1.64 | 2.08 | 2.74 | 3.40 |
| $\langle \tilde{a}^2 \rangle$ | 2.63 | 1.89 | 1.65 | 1.45 | 1.38 | 1.29 | 1.21 | 1.14 | 1.08 | 1.03 | 0.98 | 0.89 | 0.80 | 0.68 | 0.54 | 0.45 |
| $\langle \tilde{a}^4 \rangle$ | 133 | 32.9 | 21.6 | 16.3 | 13.1 | 10.9 | 9.29 | 8.03 | 7.01 | 6.18 | 5.48 | 4.37 | 3.36 | 2.23 | 1.39 | 0.90 |
| $St^{(c)}$ | 0 | 0.16 | 0.26 | 0.37 | 0.47 | 0.58 | 0.68 | 0.79 | 0.89 | 1.00 | 1.10 | 1.31 | 1.57 | 1.99 | 2.62 | 3.25 |
| $\langle \tilde{a}^2 \rangle$ | 2.02 | 1.59 | 1.40 | 1.28 | 1.19 | 1.11 | 1.05 | 0.99 | 0.94 | 0.89 | 0.85 | 0.77 | 0.70 | 0.59 | 0.47 | 0.39 |
| $\langle \tilde{a}^4 \rangle$ | 52.8 | 19.1 | 13.1 | 10.1 | 8.24 | 6.95 | 6.01 | 5.24 | 4.61 | 4.11 | 3.67 | 2.95 | 2.32 | 1.59 | 0.97 | 0.63 |

TABLE 2. Normalised values of the second and fourth moments of the acceleration $\langle \tilde{a}^2 \rangle = \langle \mathbf{a}^2 \rangle / [3(\epsilon^3/\nu)^{1/2}]$, $\langle \tilde{a}^4 \rangle = \langle \mathbf{a}^4 \rangle / [3(\epsilon^3/\nu)]$ for ^(a) $R_\lambda = 185$, ^(b) $R_\lambda = 105$ and ^(c) $R_\lambda = 65$. The statistical error on all entries are of the order of 5%.

that at increasing Stokes the two curves start to deviate from each other, the tracer acceleration conditioned on the particle positions has a minimum for $St \approx 0.5$ close to the maximum of clustering (see inset of Fig. 1a), eventually recovering the value of a_{rms} of the unconditioned tracers for larger St . The latter effect is a clear indication that inertial particles explore the small scale structures of the flow more and more homogeneously by increasing St . In this limit a different mechanism is responsible for the reduction of the a_{rms} .

At large St , i.e. $\tau_s \gg \tau_\eta$, the inspection of Eq. (3.2) shows that the main effect of inertia on particle acceleration is a low-pass filtering of fluid velocity differences, with a suppression of fast frequencies above τ_s^{-1} . In figure 1b we also compare the acceleration variance with the one obtained by an artificial low-pass filtering based only on the fluid tracers trajectories. For each tracer trajectory, $\mathbf{x}(t)$, we define a new velocity, \mathbf{u}^F , filtered on a window-size of the same order of the Stokes time:

$$\mathbf{u}^F(t) = \frac{1}{\tau_s} \int_{-\infty}^t e^{-(t-s)/\tau_s} \mathbf{u}(\mathbf{x}(s), s) ds \quad (3.3)$$

The filtered acceleration is thus given by $\mathbf{a}^F = \frac{d}{dt} \mathbf{u}^F$. Of course, in order to extract the effect due to filtering only we are compelled to employ fluid trajectories: (3.3) applied along particle trajectories is nothing but Eq. (3.1), so that the acceleration would coincide with the particle acceleration by definition. The root mean square fluctuation, $a_{\text{rms}}^F = \langle (\frac{d}{dt} \mathbf{u}^F)^2 \rangle^{1/2}$, is thus computed by averaging along the tracer trajectories without any condition on their spatial positions, i.e. homogeneously distributed in the whole $3d$ domain. The curves corresponding to a_{rms} and to a_{rms}^F become closer and closer as St grows larger, supporting the conjecture that preferential concentration for $St > 1$ becomes less important. For intermediate St we expect a non trivial interplay between the two above mechanisms that makes very difficult to build up a model able to reproduce even the qualitative behaviour.

Another interesting aspect shown in Fig. 1a is the residual dependence of the normalised particle acceleration on Reynolds number. For the case of fluid tracers it is known that intermittent corrections to the dimensional estimate $a_{\text{rms}} = a_0(\epsilon^3/\nu)^{1/4}$ may explain the Reynolds dependence (Sawford *et al.* 2003, Hill 2002, Biferale *et al.* 2004). Data suggest that the fluid intermittency may be responsible of such deviations at $St > 0$ as well.

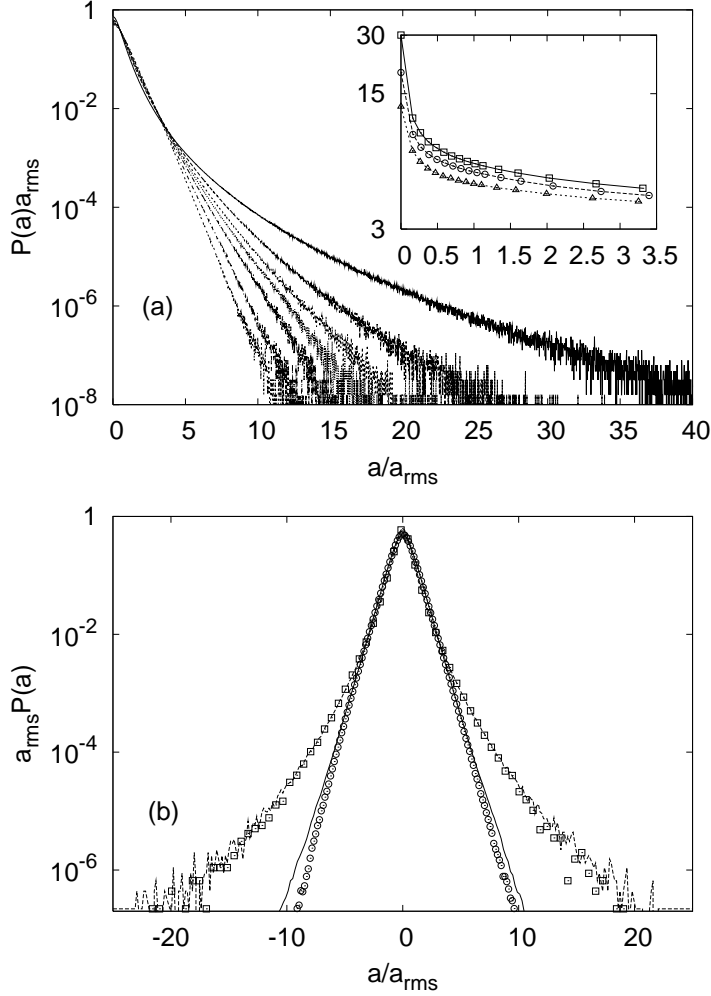


FIGURE 2. (a) Acceleration pdf's for a subset of Stokes values ($St = 0, 0.16, 0.37, 0.58, 1.01, 2.03, 3.31$ from top to bottom) at $R_\lambda = 185$. The inset displays the acceleration flatness, $\langle a^4 \rangle / \langle a^2 \rangle^2$, at increasing R_λ from bottom to top. (b) The two more external curves correspond to the acceleration pdf for $St = 0.16$ (\square) and the pdf of the fluid tracers acceleration measured on the same position of the inertial particles, $\frac{Du}{Dt}$ (solid line). The two inner curves are the acceleration pdf at the highest Stokes, $St = 3.31$, (\circ) and the pdf of the filtered fluid acceleration (solid line). All curves are normalised to have unit variance.

This view is supported by the fact that the curves for the three Reynolds numbers are almost parallel.

A two-parameters formula for the variance of the acceleration as a function of Stokes number can be derived in the limit of vanishing Stokes numbers as: $a_{\text{rms}}^2(St) = a_{\text{rms}}^2(0) + C \exp[-(D/St)^\delta]$ (Falkovich 2005). This expression follows from the acceleration pdf of tracer particles under the assumptions that (i) the main effect of inertia is to reduce the particle concentration in regions where the accelerations is larger than $\nu^{1/2}/\tau_s^{3/2}$; (ii) the pdf tail is well reproduced by a stretched exponential shape with exponent $\beta = 2/3\delta$. Although the formula fits well the data, the limitation of our data-set to only a few points with $St \ll 1$ does not permit a significant benchmark of the model.

In table 2 we summarise the values that we have measured for $\langle \mathbf{a}^2 \rangle$ and $\langle \mathbf{a}^4 \rangle$ as a function of all Stokes and for all Reynolds numbers available. Besides the effect of inertia on typical particle accelerations it is also interesting to investigate the effects on the form of the probability distribution function $\mathbf{a}(t)$. As shown in Fig. 2a, the pdf's get less and less intermittent as St increases. In the inset of the same figure we show the flatness, $\langle \mathbf{a}^4 \rangle / \langle \mathbf{a}^2 \rangle^2$, as a function of St . The abrupt decreasing for $St > 0$ is even more evident here (notice that the y scale is logarithmic).

In the limits of small and large St the qualitative trend of the pdf's can be captured by the same arguments used for a_{rms} . In Fig. 2b we compare the pdf shape for the smallest Stokes number with the one obtained by using the tracer acceleration measured on the particle position, $\frac{D\mathbf{u}}{Dt}$. As one can see the two functions overlap perfectly, confirming that the only difference between fluid particles and inertia particles for small Stokes is due to preferential concentration. In the same figure we also compare for the highest Stokes, $St = 3.31$, the pdf of the particle acceleration with the one obtained from the filtered fluid trajectories. Now the agreement is less perfect but still fairly good, reassuring that this limit can be captured starting from a low-pass filter of fluid tracer velocities. It is worth mentioning that the pdf of tracer acceleration measured on the particle position, $\frac{D\mathbf{u}}{Dt}$, approaches the unconditioned pdf as St increases (not shown). This further confirms that preferential concentration has a minor role on the acceleration at these large Stokes values.

4. Statistics of acceleration conditioned on the flow topology

We now focus on particle acceleration statistics conditioned on the topological properties of carrier flow at particle positions. In particular, we look at the sign of the discriminant (see e.g. Chong, Perry & Cantwell 1990 and Bec 2005):

$$\Delta = \left(\frac{\det[\hat{\sigma}]}{2} \right)^2 - \left(\frac{\text{Tr}[\hat{\sigma}^2]}{6} \right)^3, \quad (4.1)$$

being $\hat{\sigma}_{ij} = \partial_i u_j$ the strain matrix evaluated at the particle position \mathbf{X} . Note that, in deriving (4.1), we omitted the term proportional to $\text{Tr}[\hat{\sigma}]$ because of incompressibility. For $\Delta \leq 0$ the strain matrix has 3 real eigenvalues (strain dominated regions), for $\Delta > 0$ it has a real eigenvalue and 2 complex conjugate ones (rotational regions). For a similar study, using a different characterisation of the flow structures, see also (Squires & Eaton 1991). Note that in two-dimension the equivalent of Δ is the well known Okubo-Weiss parameter that discerns elliptic from hyperbolic regions of the flow.

In Figs. 3a,b,c we show the acceleration pdf, $P(a|\Delta)$, conditioned on the sign of Δ at particle positions, for three different characteristic Stokes numbers $St = 0.16, 0.48, 1.34$. In Fig 3d we show the root mean squared acceleration, $\sqrt{\langle a^2 | \Delta \rangle / 3}$, as a function of St . A few results are worth to be commented. The fraction of particles in the two regions ($N(\Delta \geq 0)$) varies considerably as a function of the Stokes number (see inset of Fig. 3d), with a depletion of particles in the regions with some degree of rotation, which however becomes less effective at large St . This is similar to what is observed in the inset of Fig. 1a, where the non-homogeneous particle distribution is characterised in terms of the correlation dimension (Bec *et al.* 2005). Further, despite the shape of the pdf for a given Stokes number does not change much as a function of the sign of Δ , a noticeable change in the squared acceleration is observed. As shown in Fig. 3d, the acceleration is higher in the strain dominated regions than in the ones with some degree of rotation. We remark that the effect of inertia is dramatic: for the smallest St the conditional acceleration is larger when $\Delta < 0$ while the opposite behaviour is observed for tracer ($St = 0$). This

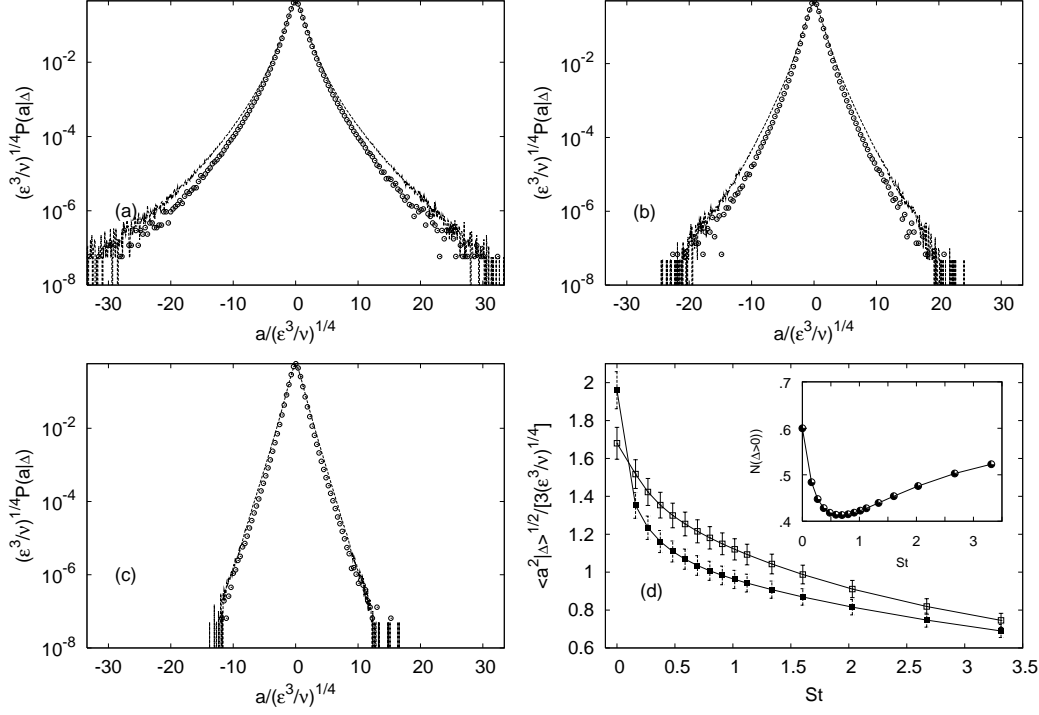


FIGURE 3. Acceleration statistics conditioned on the sign of the discriminant Δ defined in (4.1). (a) Pdf of acceleration for $St = 0.16$ conditioned on strain regions (solid line, $\Delta \leq 0$) and on rotating regions (points, $\Delta > 0$) regions, respectively. (b) and (c) same as (a) for $St = 0.48$ and $St = 1.34$. (d) Normalised root mean square conditional acceleration on $\Delta \leq 0$ (empty boxes) and $\Delta > 0$ (full boxes) regions as a function of St . The inset displays the fraction of particles in the rotating regions $N(\Delta > 0)$ ($N(\Delta \leq 0) = 1 - N(\Delta > 0)$) as a function of St . The conditional acceleration was computed on the data recorded at frequency $10\tau_\eta$ (see table 1). For $St = 0$ the acceleration $\sqrt{\langle a^2 | \Delta \rangle / 3}$ is estimated by using the pressure gradient $-\nabla p$.

may be the signature of the expulsion of particles out of intense vortex filaments (which is more effective for $St \ll 1$) leading to an undersampling of the acceleration in the regions dominated by rotational motion. The same difference is also measured for higher moments of the conditioned acceleration (not shown).

These results point out that the strong correlation between flow structure and particle preferential concentration is more effective at low Stokes numbers. At larger St the particle fraction $N(\Delta \geq 0)$ approaches the tracer value (the response time is too large to maintain the correlation between particle trajectories and the local flow topology) and the depletion of acceleration should be ascribed to the effect of filtering, as discussed in the previous section (*cfr.* Fig. 1b and 2b).

5. Conclusions and perspectives

A systematic study of the acceleration statistics of heavy particles in turbulent flows, at changing both Stokes and Reynolds numbers has been presented. The main conclusions are (i) preferential concentration plays an *almost singular* role at small Stokes. Indeed, even a quite small inertia may suffice to expel particles from those turbulent regions (vortex cores) where the most intermittent and strong acceleration fluctuations would

have been experienced; (ii) for small Stokes, a good quantitative agreement between the inertial particle acceleration and the conditioned fluid tracer acceleration is obtained; (iii) at large Stokes, the main effects is filtering of the velocity induced by the response Stokes times. For $St > 1$, the statistical properties of fluid tracers averaged over a time window of the order of τ_s are in a quite good agreement with the inertial particle properties.

Some important questions remain open.

It is not clear how to build up a phenomenological model that is able to describe the inertial particles acceleration as a function of both Stokes and Reynolds numbers. For example, a naive generalisation of the multifractal description, successfully used for fluid tracers (Biferale *et al.* 2004), may be insufficient. In fact, it is not straightforward to include in such models the correlation between preferential concentration and the local topological properties of the carrier flow. Here such correlations have been studied in terms of the real or complex nature of the eigenvalues of the strain matrix at particle positions. We found that, more effectively at small St with respect to larger St values, particles preferentially concentrate in strain dominated regions and that this preferential concentration has a clear role in determining the acceleration fluctuations. However, this information does not directly bring to a model for the acceleration statistics.

The strong fluctuations of both Kolmogorov time and Kolmogorov dissipative scale are certainly the most interesting aspects which distinguish the statistics of heavy particles in turbulence from the one measured in smooth flows. It would be then important to study also the statistical properties conditioned to the local Stokes number (defined in terms of a “local” energy dissipation, see e.g. Collins & Keswani 2004) .

Work in this direction will be reported elsewhere.

We acknowledge useful discussions with G. Falkovich, E. Bodenschatz and Z. Warhaft. This work has been partially supported by the EU under the research training network HPRN-CT-2002-00300 “Stirring and Mixing”. Numerical simulations have been performed thanks to the support of CINECA (Italy) and IDRIS (France) under the HPC-Europa project. We thank also the “Centro Ricerche e Studi Enrico Fermi” and N. Tantalo for support on the numerical computations.

REFERENCES

- BALKOVSKY, E. FALKOVICH, G. & FOUXON, A. 2001 Intermittent distribution of inertial particles in turbulent flows. *Phys. Rev. Lett.* **86**, 2790–2793.
- BEC, J. 2005 Multifractal concentrations of inertial particles in smooth random flows. *J. Fluid Mech.* **528**, 255–277.
- BEC, J. CELANI, A. CENCINI, M. & MUSACCHIO, S. 2005 Clustering and collisions of heavy particles in random smooth flows. *Phys. Fluids* **17**, 073301.
- BEC, J. GAWEDZKI, K. & HORVAI, P. 2004 Multifractal clustering in compressible flows. *Phys. Rev. Lett.* **92**, 224501.
- BIFERALE, L. BOFFETTA, G. CELANI, A. DEVENISH, B.J. LANOTTE, A. & TOSCHI, F. 2004 Multifractal statistics of Lagrangian velocity and acceleration in turbulence. *Phys. Rev. Lett.* **93**, 064502.
- BIFERALE, L. BOFFETTA, G. CELANI, A. LANOTTE, A. & TOSCHI, F. 2005 Particle trapping in three-dimensional fully developed turbulence. *Phys. Fluids* **17**, 021701.
- BOFFETTA, G. DE LILLO, F. & GAMBA, A. 2004 Large scale inhomogeneity of inertial particles in turbulent flows. *Phys. Fluids* **16**, L20–L24.
- BOIVIN, M. SIMONIN, O. & SQUIRES, K.D. 1998 Direct numerical simulation of turbulence modulation by particles in isotropic turbulence. *J. Fluid Mech.* **375**, 235–263.
- CHEN, S. DOOLEN, G.D. KRAICHNAN, R.H. & SHE, Z.S. 1993 On statistical correlations between velocity increments and locally averaged dissipation in homogeneous turbulence. *Phys. Fluids A* **5**, 458–463.

- CHONG, M.S., PERRY, A.E. & CANTWELL, B.J. 1990 A general classification of three-dimensional flow field. *Phys. Fluids A* **2**, 765–777.
- CHUN, J. KOCH, D.L. RANI, S. AHLUWALIA, A. & COLLINS, L.R. 2005 Clustering of aerosol particles in isotropic turbulence. *J. Fluid Mech.* **536**, 219–251.
- COLLINS, L.R. & KESWANI, A. 2004 Reynolds number scaling of particle clustering in turbulent aerosols. *New J. Phys.* **6**, 119.
- CSANADY, G. 1980 *Turbulent diffusion in the environment*. Geophysics and Astrophysics Monographs Vol. 3 D. Reidel Publishing Company.
- EATON, J.K. & FESSLER, J.R. 1994 Preferential concentrations of particles by turbulence. *Int. J. Multiphase Flow* **20**, 169–209.
- FALKOVICH, G. FOUXON, A. & STEPANOV, M. 2002 Acceleration of rain initiation by cloud turbulence. *Nature* **419**, 151–154.
- FALKOVICH, G. & PUMIR, A. 2004 Intermittent distribution of heavy particles in a turbulent flow. *Phys. Fluids* **16**, L47–L51.
- FALKOVICH, G. 2005 Private Communication.
- HILL, R.J. 2002 Scaling of acceleration in locally isotropic turbulence. *J. Fluid Mech.* **452**, 361–370.
- LA PORTA, A. VOTH, G.A. CRAWFORD, A.M. ALEXANDER, J. & BODENSCHATZ, E. 2001 Fluid particle accelerations in fully developed turbulence. *Nature* **409**, 1017–1019.
- LA PORTA, A. VOTH, G.A. CRAWFORD, A.M. ALEXANDER, J. & BODENSCHATZ, E. 2002 Measurement of particle accelerations in fully developed turbulence. *J. Fluid Mech.* **469**, 121–160.
- LEWIS, D. & PEDLEY, T. 2000 Planktonic contact rates in homogeneous isotropic turbulence: Theoretical predictions and kinematic simulations. *J. Theor. Biol.* **205**, 377–408.
- MAXEY, M.R. & RILEY, J. 1983 Equation of motion of a small rigid sphere in a nonuniform flow. *Phys. Fluids* **26**, 883–889.
- MORDANT, N. METZ, P. MICHEL, O. & PINTON, J.-P. 2001 Measurement of Lagrangian velocity in fully developed turbulence. *Phys. Rev. Lett.* **87**, 214501.
- PINSKY, M. & KHAIN, A. 1997 Turbulence effects on droplet growth and size distribution in clouds—a review. *J. Aerosol Sci.* **28**, 1177–1214.
- POST, S. & ABRAHAM, J. 2002 Modeling the outcome of drop-drop collisions in Diesel sprays. *Int. J. of Multiphase Flow* **28**, 997–1019.
- READE, W.C. & COLLINS, L.R. 2000 A numerical study of the particle size distribution of an aerosol undergoing turbulent coagulation. *J. Fluid Mech.* **415**, 45–64.
- ROTHSCHILD, B.J. & OSBORN, T.R. 1988 Small-scale turbulence and plankton contact rates. *J. Plankton Res.* **10**, 465–474.
- SAWFORD, B.L. & GUEST, F.M. 1991 Lagrangian statistical simulation of the turbulent motion of heavy particles. *Boundary-Layer Meteorol.* **54**, 147–166.
- SAWFORD, B.L. YEUNG, P.K. BORGAS, M.S. VEDULA, P. LA PORTA, A. CRAWFORD, A.M. BODENSCHATZ, E. 2003 Conditional and unconditional acceleration statistics in turbulence. *Phys. Fluids* **15**, 3478–3489.
- SEINFELD J. 1986 *Atmospheric chemistry and physics of air pollution*. J. Wiley and Sons.
- SHAW, R.A. 2003 Particle-turbulence interactions in atmospheric clouds. *Ann. Rev. Fluid Mech.* **35**, 183–227.
- SQUIRES K.D. & EATON J.K. 1991 Preferential concentration of particles by turbulence. *Phys. Fluids A* **3**, 1169–1178.
- VILLEDIEU P. & HYLKEMA J. 2000 Modèles numériques lagrangiens pour la phase dispersée dans les propulseurs à poudre. Rapport technique ONERA.
- WARHAFT, Z. GYLFASON, A. & AYYALASOMAYAJULA, S. 2005 private communication.
- ZAICHIK, L.I. SIMONIN, O. & ALIPCHENKOV V.M. 2003 Two statistical models for predicting collision rates of inertial particles in homogeneous isotropic turbulence. *Phys. Fluids* **15**, 2995–3005.
- ZHOU, Y. WEXLER, A. & WANG, L.-P. Modelling turbulent collision of bidisperse inertial particles. *J. Fluid Mech.* **433**, 77–104.